ACS APPLIED MATERIALS & INTERFACES

Research Article

www.acsami.org

Ultrahigh Responsivity and External Quantum Efficiency of an Ultraviolet-Light Photodetector Based on a Single VO_2 Microwire

Jyh Ming Wu* and Wei En Chang

Department of Materials Science and Engineering, National Tsing Hua University, 101, Section 2 Kuang Fu Road, Hsinchu 300, Taiwan

Supporting Information

ABSTRACT: We demonstrated a single microwire photodetector first made using a VO_2 microwire that exhibted high responsivity (R_λ) and external quantum efficiency (EQE) under varying light intensities. The VO_2 nanowires/microwires were grown and attached on the surface of the SiO_2/Si(100) substrate. The SiO_2 layer can produce extremely low densities of long VO_2 microwires. An individual VO_2 microwire was bonded onto the ends using silver paste to fabricate a photodetector. The high-resolution transmission electron microscopy image indicates that the nanowires grew along the [100] axis as a single crystal. The critical parameters, such as R_λ, EQE, and detectivity, are extremely high, 7069 A W^{-1}, 2.4 × 10^{10}%, and 1.5 × 10^{14} Jones, respectively, under a bias of 4 V and an illumination intensity of 1 μW cm^{-2}. The asymmetry in the $I-V$ curves results from the unequal barrier heights at the two contacts. The photodetector has a linear $I-V$ curve with a low dark current while a nonlinear curves was observed under varing light intensities. The highly efficient hole-trapping effect contributed to the high responsivity and external quantum efficiency in the metal−oxide nanomaterial photodetector. The responsivity of VO_2 photodetector is 6 and 4 orders higher than that of graphene (or MoS_2) and GaS, respectively. The findings demonstrate that VO_2 nanowire/microwire is highly suitable for realizing a high-performance photodetector on a SiO_2/Si substrate.

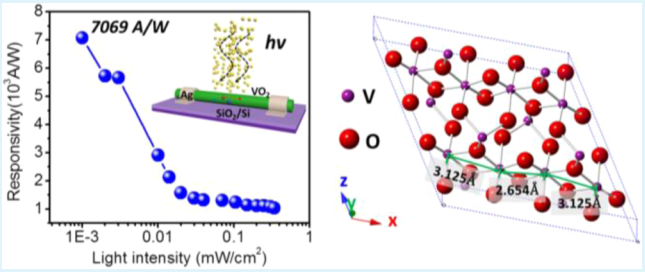

KEYWORDS: *VO_2, photodetector, quantum efficiency, responsivity, detectivity*

1. INTRODUCTION

Narrow band gap (i.e., 0.7 eV) vanadium dioxide (VO_2) has a unique property, undergoing a metal−insulation transition (MIT) at a temperature of ∼68 °C.[1,2] The VO_2 possesses unique electrical and optical properties that point to promising applications in optical switching,[3] electrochromic devices,[4] and energy-saving smart windows.[2,5] Recently, photodetectors made from ZnO,[6−10] GaN/AlN,[11] SnO_2,[12] and $ZnSnO_3$[13] have been systematically reported; however, constructing detectors possessing high detectivity, low noise, and high responsivity is still considered a challenging task. Therefore, two-dimensional (2D) monolayer nanomaterials such as graphene,[14] MoS_2,[15,16] and GaS,[17] have attracted increasing attention because of their unique electrical properties in the applications of the optoelectronic nanodevices. However, the choice of substrate is critical for the synthesis of the monolayer 2D materials,[18] and graphene lacks a band gap around the Fermi level; therefore, many techniques have been addressed to investigate the band gap opening issue of graphene.[19,20]

A nanowire photoconductor can yield a higher light sensitivity than bulk material.[21,22,13] Moreover, heterojunction nanowire is capable of sensing and amplifying an output signal (i.e., photocurrent) with high responsivity and sensitivity.[23] Therefore, heterojunction nanomaterials, such as GaN/AlN,[24] Ge/Si,[23] P3HT:ZnO,[25] graphene/PbS quantum dot,[26] and ZnS−ZnO,[27] have significantly been attractive to improve the critical parameters of photodetectors, for instance, quantum efficiency, responsivity, detectivity, and sensitivity.[28,29] Recently, researchers are now focusing on the building blocks of branched heterostructures that may be promising candidates for UV photodetector sensors,[27,30] but these materials have increased the complexity of the procedures. Moreover, the high-performance nanowire-based photodetectors generally need a higher crystallinity. During the crystal growth process, the occurrence of natural defects[31] could induce defective states,[32] which are responsible for the slow decay of the photocurrent in the dark state and for the weak light intensity dependence of the photocurrent.[33]

In this work, single crystal VO_2 nanowires/microwires were randomly grown on a SiO_2/Si(100) substrate at a temperature of 800 °C.[2] The VO_2 photodetector exhibited an excellent response for ultraviolet light (wavelength, λ ∼ 360−400 nm). The responsivity (R_λ), external quantum efficiency (EQE), and detectivity of VO_2 photodetector are 7069 A W^{-1}, 2.4 × 10^{10}%, and 1.5 × 10^{14} Jones, respectively, which are strongly dependent on UV-light intensity. The high-performance

Received: June 7, 2014
Accepted: July 16, 2014
Published: July 16, 2014

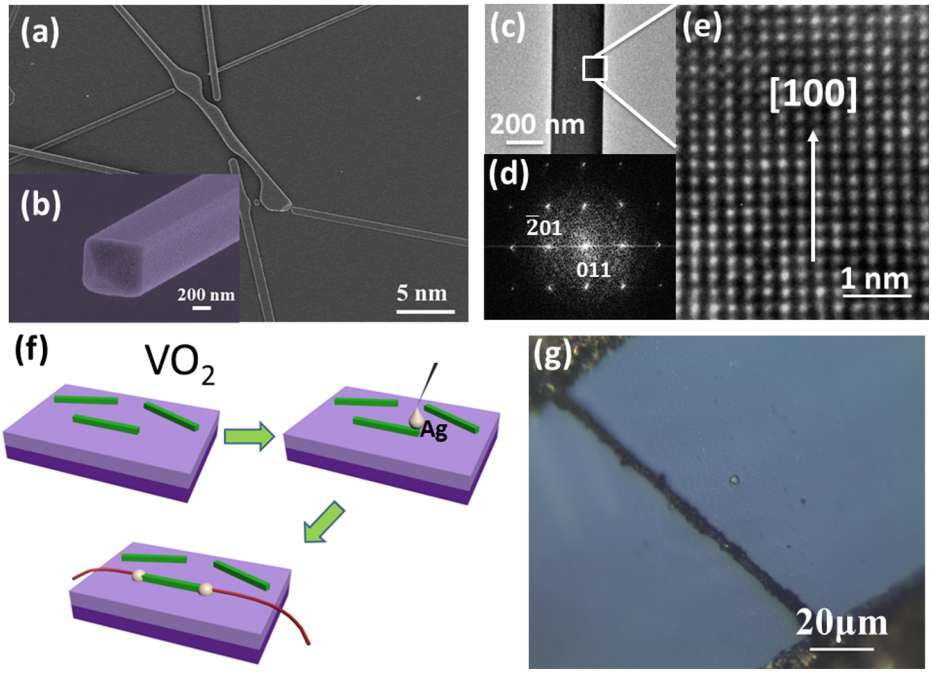

Figure 1. (a) FESEM image of VO_2 nanowires/micorwires, (b) cross-sectional VO_2 nanowire with diameter ~200−800 nm. (c) TEM image of an individual VO_2 nanowire. (d) SAD pattern showing the side facet bound by (011) and ($\bar{2}$01). (e) HRTEM image showing the nanowires' growth direction of the [100] axis. (f) The fabrication process of an individual VO_2 microwire photodetector. (g) A digital optical microscope image of a VO_2 microwire.

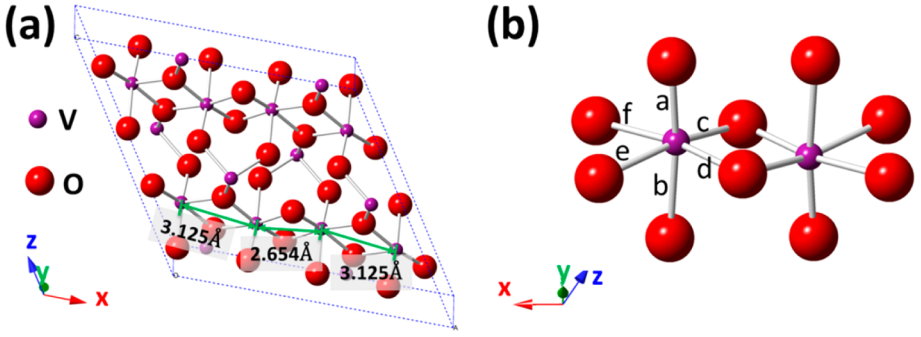

Figure 2. (a) Crystallographic structure of monoclinic VO_2 showing a distorted alternative distances at 3.125 and 2.654 Å. (b) Two symmetric octahedral cells with bonding length of a, b, c, d, e, and f (see details in the text).

ultraviolet-light photodetector is first made by a single VO_2 microwire on a SiO_2/Si substrate. The responsivity and external quantum efficiency of the VO_2 photodetector are respectively ca. 6 and 4 orders higher than those of 2D materials such as graphene,[34] MoS_2,[35] GaSe,[36] and GaS.[17] To the best of our knowledge, this work is the first demonstration of the high responsivity and EQE for a single VO_2 microwire in metal−oxide materials, confirming VO_2 as a prospective material for efficient optoelectronic devices.

2. EXPERIMENTAL METHOD

Material Preparation. The VO_2 nanowires/microwires were synthesized on SiO_2(100 nm)/p-type Si(100) substrates by the vapor transfer process. The source materials of V_2O_5 (1 g, Prochem, purity 99%) and SiO_2/Si substrates were placed on an alumina crucible and then loaded into the middle of a quartz tube in a horizontal furnace system. A flow of argon gas (10 sccm, purity 99.99%) was introduced into the reactor for 3 h, and the working pressure was controlled at 8 Torr with a temperature of 800 °C.

Device Fabrication. After the VO_2 nanowires/microwires were synthesized onto the SiO_2/Si substrate, the silver paste was carefully bonded onto the ends of the VO_2 microwire to fabricate a single microwire metal−semiconductor−metal (MSM) photodetector.

Material Characterization. The material characterizations were conducted by using an X-ray diffractometer (Burker D8SSS), field emission scanning electron microscope (FESEM, Hitachi S-4800), and high-resolution transmission electron microscope (HRTEM, JEOL JEM-3000F). Micro-Raman spectroscopy measurement was carried out at room temperature with backscattering geometry using a Dilor X-Y modular laser.

Electrical Measurement. UV light with varying light intensity (I = 1 μW cm^{-2} to 0.41 mW cm^{-2}, wavelength λ ~ 360−400 nm) was used as the excitation light-source with the electrical measurement systems of a Stanford function generator (DS340) and a Stanford current-meter (SR-570), to characterize the transient photoresponsive properties of the VO_2 photodetector.

3. RESULTS AND DISCUSSION

Figure 1a shows that the VO_2 nanowires/microwires were grown on SiO_2/p-Si(100) substrate, and the nanowires/microwires were around several hundred micrometers long. The diameter of the VO_2 nanowires was in the range of 200−

dx.doi.org/10.1021/am503598g | ACS Appl. Mater. Interfaces 2014, 6, 14286−14292

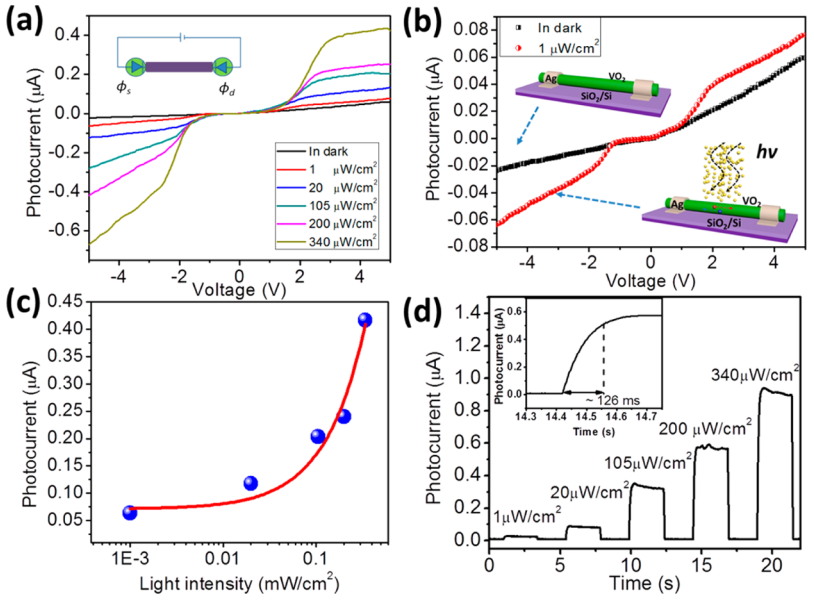

Figure 3. (a) The $I-V$ characteristic curves under illumination of the different UV intensities (from 0 to 340 μW cm^{-2}. (b) Linear $I-V$ (in the dark state) and nonlinear $I-V$ curves (under UV illumination) for MSM Schottky contact interfaces. (c) Photocurrent as a function of different intensities of UV illumination. (d) Photocurrent is measured at 4 V under different UV illumination intensities, such as 1, 20, 105, 200, and 340 μW/cm^2; inset image is the response time.

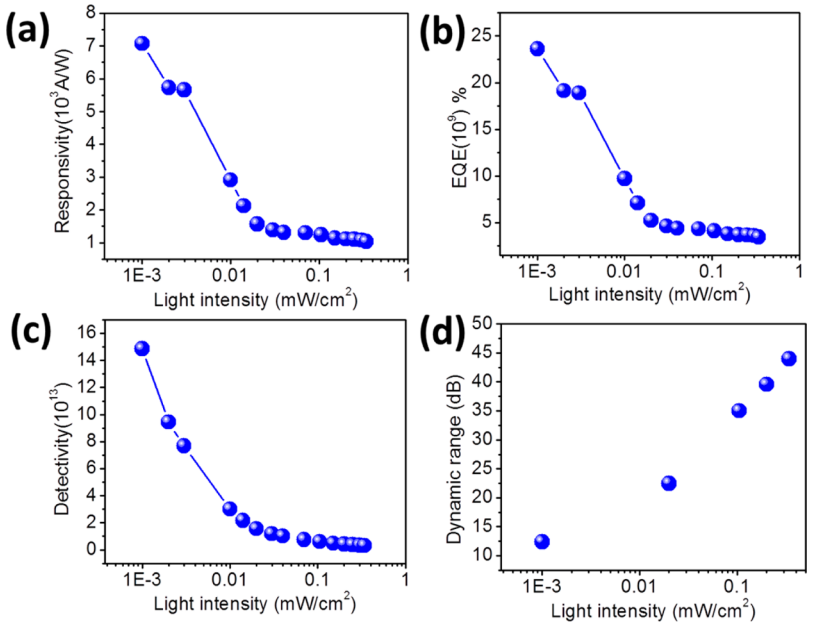

Figure 4. Critical parameters of UV photodetector such as (a) responsivity, (b) EQE, (c) detectivity, and (d) linear dynamic range as a function of varying light intensity.

800 nm, as shown in Figure 1b. Parts c and d of Figure 1display a low-magnification TEM image of a VO_2 nanowire and the corresponding selected area electron diffraction (SAED) pattern, respectively, indicated that the VO_2 nanowires with the zone axis [1$\bar{2}$2], are grown along the [100] direction, which is vertical to the ($\bar{2}$01) plane. The lattice fringes of adjacent planes ~0.28 nm correspond to the VO_2(011) plane (see Figure 1e).[37] The XRD pattern and Raman specctrum of VO_2 nanowires/microwires are shown in the Supporting Information (Figures S1 and S2, respectively). The XRD pattern and Raman spectrum have demonstrated that the VO_2 microwires belongs to a monoclinic structure. The schematic diagram in Figure 1f shows the fabrication process of a single microwire VO_2 photodetector. First, the VO_2 microwires were randomly grown and attached to a SiO_2/p-Si substrate. Next, the silver paste was bonded onto the end of the VO_2 microwire to fabricate a photodetector.[38,39] The optical microscope image in Figure 1g reveals that the VO_2 microwire (with a length of ~130 μm) was successfully bonded by the silver electrode.

The VO_2 is a symmetry of monoclinic structure.[40] Figure 2a shows a crystallographic structure of VO_2 with the space group of $P2_1/c$. The parameters of the monoclinic unit cell are a = 5.743 Å, b = 4.517 Å, c= 5.375 Å, and β = 122.65°. In the multiunit cell of the monoclinic structure, the V−V chains

along x axis becomes distorted with alternative distances of 2.654 and 3.125 Å.[41] Figure 2b further shows the two types of distorted octahedra cells. The bonding length of V−O chain, as labeled by a, b, c, d, e, and f, are 1.762, 2.051, 1.872, 1.860, 2.008, and 2.033 Å, respectively. Thus, the vanadium(V) atom does not position itself in the center of the symmetry octahedral cell of the monoclinic structure.

Figure 3a reveals that the I−V curves were characterized by varying light intensity (from 0 to 340 μW cm^{-2}). The asymmetry in the I−V curves result from the unequal Schottky barrier heights at the two contacts. Under both positive and negative bias, the photocurrent of the photodetector increases upon increasing the light intensity. Figure 3b further shows that an almost linear I−V characteristic curve was measured under dark conditions, while a nonlinear I−V curve formed under illumination of light intensity ∼1 μW cm^{-2}. The electronic model of VO_2 photodetector can be regarded as a single microwire sandwiched between two back-to-back Schottky diodes. Figure 3c reveals that the photocurrent is proportional to the UV-light intensity with a natural logarithmic. To evaluate the response time, the sample was irradiated under a varying light intensity from 1 to 340 μW cm^{-2} with a constant bias of 4 V. Figure 3d reveals that the photocurrent instantly increases to reach an equilibrium state and then immediately drops to its original state, as the UV light is turned on and turned off, respectively. The corresponding response time is ∼126 ms, which was taken by the device to reach 90% of the maximum photocurrent (see the inset in Figure 3d).[42]

Parameters such as responsivity (R_λ), external quantum efficiency (EQE), and detectivity are critical factors when evaluating the optical properties of the photodetector. The responsivity (R_λ) can be expressed as eq 1.[17]

$$R_\lambda = \frac{\Delta I}{pA} \tag{1}$$

R_λ is defined as the photocurrent yield per unit power density of the incident light on the effective area "A" of a VO_2 microwire, ΔI is the photoexcited current, which is obtained by fitting the measured data, and p denotes the light intensity that illuminates the surface of the VO_2 microwire. Figure 4a shows that the R_λ is 7069 A W^{-1} as the photodetector was operated under 4 V external bias. The calculated responsivity of the photodetector is extremely high, under an illumination of light intensity ∼1 μW/cm^2. Such a result gives a high on/off switching ratio, demonstrating that the high performance of the VO_2 photodetector is potentially useful in the UV spectral region. We suggested that the high responsivity is ascribed to the hole-trapping effect of the surface of the microwire. Namely, more photogenerated holes were trapped by adsorbed oxygen species on the surfaces of microwire, inhibiting the recombination of excitons under UV illumination and contributed a significant photocurrent.[43,44] In contrast, the responsivity is significantly decreased at a relatively high UV-light intensity because of the saturation of the hole-trapping effect and the increasing recombination of photogenerated electron−hole pairs (see details below).[45]

To rule out the effective change of the incident photon flux on the photocurrent, EQE is a useful physical quantity to evaluate the photodetector's electrical sensitivity to UV light. The EQE was used to determine the number of photoinduced carriers per incident photons, as shown in eq 2.

$$\mathrm{EQE} = \frac{R_\lambda hc}{\lambda e} \tag{2}$$

where h is Planck's constant, c represents the velocity of light, λ denotes the light wavelength, and e is the electron charge. Figure 4b reveals that the EQE decreases from 2.4 × 10^{10}% to 3.5 × 10^9% upon decreasing the light density from 1 μW cm^{-2} to 0.41 mWcm^{-2}, respectively. The higher responsivity and EQE indicated that higher excitation energy improves the photoelectric conversion.[17] The detectivity (d^*, in units of Jones) can be expressed by eq 3

$$d^* = \frac{R_\lambda S^{1/2}}{(2eI_{\mathrm{dark}})^{1/2}} \tag{3}$$

where S is considered as the effective area of the photodetector. In this work, the d^* value is in the range from 1.5 × 10^{14} to 3 × 10^{12} Jones (bandwidth ∼ 0.4 Hz), as shown in Figure 4c. The detectivity decreases by lowering the light intensity. The detectivity is attractive and can be comparable with the silicon diodes[46] and InGaAs (d^* ∼ 10^{12}). Table 1 summarizes the critical parameters of the VO_2 photodetector and compares heterojunction nanomaterials and two-dimensional (2D) materials.[11,17,25,30,47,48] The excellent R_λ in the VO_2 photodetector is ∼6 orders higher than that of graphene (R_λ ∼ 1 × 10^{-3} A W^{-1}, on SiO_2/Si)[34] and MoS_2 (R_λ ∼ 7.5 × 10^{-3} A W^{-1}, on SiO_2/Si)[35] and 4 orders higher than that of GaSe (R_λ ∼ 2.8 A W^{-1}, on SiO_2/Si)[36] and GaS (R_λ ∼ 4.2 A W^{-1}, on SiO_2/Si).[17] On the basis of our experimental results, the VO_2 photodetector revealed an extremely high responsivity, external quantum efficiency, and detectivity. This is the first finding of the high performance of a photodetector made from a single VO_2 microwire. The critical parameters of the VO_2 photodetector, such as responsivity and EQE, are extremely high based on metal−oxide materials to date. Figure 4d shows that the linear dynamic range (LDR) is around 45 dB, which can be compared with GaN photodetector.[18] The low LDR can be attributed to a slightly higher dark current [(8 × 10^{-9})−(5 × 10^{-8}) A)], which will be improved in our future work. The sensitivity of the VO_2 microwire is revealed in the Supporting Information (Figure S3).

Table 1. Summary of the Critical Parameters for UV Photodetectors

materials	responsivity (R_λ, A W^{-1})	external quantum efficiency (EQE, %)	ref
GaN/AlN	2000	–	11
GaS nanosheet	4.2	20.5	17
P3HT:ZnO	1000	3.4 × 10^3	25
monolayer graphene	1 × 10^{-3}	6−16	30
GaSe	2.8	1376	36
ZnO−graphene	640	1000−1200	47
ZnO nanoparticles	731	–	48
VO_2 microwire	7069	3.6 × 10^7	this work

On the basis of the Schottky contact at the MSM interfaces, the barrier height is strongly dependent on the doping concentration and surface properties of the semiconductor. If considering that a microwire had a low impurity level, the Schottky contact with a semiconductor was by transport of electrons over the potential barrier, which can be described by a

classic thermionic emission-−diffusion equation,[19,38,49] as given by eq 4.

$$J = A^{*}\,T^{2}\exp\left(-\frac{\varphi_{b}}{kT}\right)\exp\left(\frac{\sqrt[4]{\frac{0.125N_{d}(V_{bi}+V-k_{B}T/e)}{\pi^{2}\varepsilon_{s}^{3}}}}{k_{B}T}\right) \quad (4)$$

where A^{*} is the effective Richardson constant, ϕ_b denotes the Schottky barrier height, N_d is the donor concentration, T is the temperature, e is the electron charge, V_{bi} represents the potential at the barrier, k_B denotes the Boltzmann constant, and ε_s is the permittivity of VO_2. In this case, the conductance (J) varies exponentially with the Schottky barrier height (ϕ_b). Therefore, it is reasonable to explain how the photocurrent varies exponentially with the light intensity (see Figure 3c). On the basis of eq 4, the ln I−$V^{1/4}$ curve (see Supporting Informatiom, Figure S4) is very linear (using the data provided by the black line in Figure 3a). Thus, the Schottky barrier formula can precisely explain our experimental data.

In this work, the sensing mechanism is based on the gas adsorption and desorption process near the MSM interfaces, which can be modulated by the distribution of the local electric field, leading to the detection that the photocurrent has significantly changed. The Schottky barrier height can be regarded as a blocking zone at two contacts, which can effectively tune the barrier height by UV-light illumination. As shown in Figure 5a, once the oxygen ions (negatively charged)

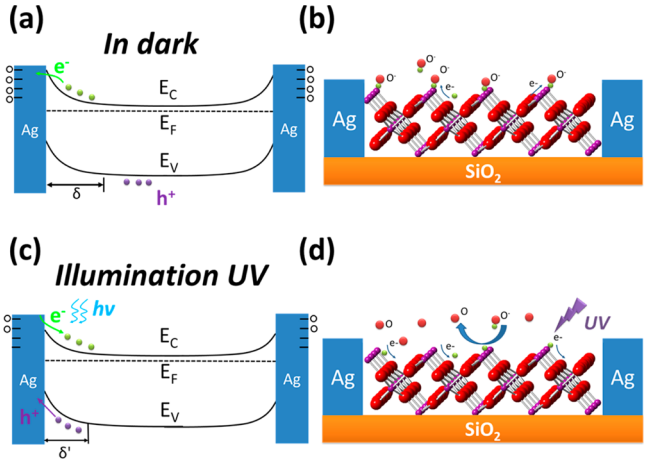

Figure 5. (a) The band structure of VO_2 in the dark state and the formation of the Schottky barriers at the MSM interface creating the depletion zones ($\sim\delta$). (b) The corresponding atomic structure, showing the oxygen ions absorbed on the surface of VO_2 crystal by capturing an electron from the VO_2 microwire. (c) The Schottky barrier width ($\sim\delta'$) at the MSM interface was reduced under UV-light irradiation. (d) The corresponding atomic structure, where the electrons were infused into the conduction band of VO_2 through recombination of oxygen ions and holes; consequently, the oxygen was released into the air and enhanced the conductance of the VO_2 microwire.

were absorbed on the surface of the microwire by capturing the electron from the conduction band of the VO_2, a depleation zone (δ) was created at the interface of the VO_2 microwire. Therefore, an almost linear I−V curve with very low dark current was obseved under dark conditions. In other words, the electrons were captured by molecular oxygen and formed a negative charge (oxygen ion), which was absorbed on the surface of the VO_2 microwire, as shown in the corresponding schematic diagram of Figure 5b. In contrast, sufficient UV-light energy falls on the depletion zone at the MSM interface, leading to a decrease of the Schottky barrier height (or width) (δ'), as shown in Figure 5c. Subsequently, electrons jump into the conduction band from the valence band and the remaining holes into the valence band. The photogenerated holes then migrate to the surface and discharge the adsorbed oxygen ions ($h^+ + O_2^- \rightarrow O_2$). The electron is therefore released from the oxygen ions and infused into the conduction band of the microwire, thereby increasing the conductance of the microwire, as shown in Figure 5d. Note that the Schottky barrier width will further decrease with the increase of the light intensity, thereby increasing the discharge of the adsorbed oxygen ions and contributing a significant photocurrent. We therefore concluded that the photocurrent passing through the Schottky contact is sensitive to the barrier height and width.[50]

In this work, the Si substrate was predeposited in a SiO_2 layer to promote the growth of the VO_2 nanowires/microwires attached on the surface of the SiO_2 surface.[51] A single VO_2 microwire was bonded onto the ends by silver paste to fabricate a photodetector. The only pathway for charge transfer is formed from one electrode to the other one.[46] Therefore, a high photocurrent can instantly be built up. This work reports the important finding that a single VO_2 nanowire/microwire can be used for a highly effective UV photodetector, which has never been discovered until now.

4. CONCLUSION

In summary, the VO_2 nanowires/microwires were grown on a SiO_2/p-Si(100) substrate at a temperature of 800 °C. An individual VO_2 microwire was bonded at its end to a Si substrate as a UV photodetector. The responsivity and EQE of the VO_2 photodetector were strongly dependent on the light intensities. By increasing the bias applied, the low dark current (in the dark state) of the photodetector increases almost linearly in the range from −5 to +5 V. As the sample was irradiated by the UV light, the photocurrent significantly increases with a nonlinear I−V curve. Under illumination by 1 μW cm^{-2}, the critical parameters for a UV photodetector, such as responsivity, external quantum efficiency, and detectivity, were discovered to be 7069 A W^{-1}, 2.4 × 10^{10}%, and 1.5 × 10^{14} Jones, respectively, at a constant low bias of 4 V. The responsivity and EQE are 6 and 4 orders higher than those of graphene (or single-layer MOS_2) and GaS (or fewer layer of GaSe), respectively. This high responsivity and external quantum efficiency of the UV-light photodetector is the first report on inorganic nanomaterials based on a single VO_2 microwire.

■ ASSOCIATED CONTENT

Supporting Information

XRD pattern, Raman spectrum, and I−V curves. This material is available free of charge via the Internet at http://pubs.acs.org.

■ AUTHOR INFORMATION

Corresponding Author

*E-mail wujm@mx.nthu.edu.tw.

Notes

The authors declare no competing financial interest.

■ ACKNOWLEDGMENTS

The authors would like to thank the National Science Council of the Republic of China for financially supporting this research under Contract Nos. NSC 100-2628-E-035-006-MY2, NSC 102-2221-E-007-146-MY3, and NSC 102-2221-E-007-147-MY3. The authors thank to Bang-Lian Liou for TEM work.

■ REFERENCES

(1) Morin, F. J. Oxides Which Show a Metal-to-Insulator Transition at the Neel Temperature. *Phys. Rev. Lett.* **1959**, *3*, 34−36.
(2) Wu, J. M.; Liou, L. B. Room Temperature Photo-Induced Phase Transitions of VO_2 Nanodevices. *J. Mater. Chem.* **2011**, *21*, 5499−5504.
(3) Rini, M.; Hao, Z.; Schoenlein, R. W.; Giannetti, C.; Parmigiani, F.; Fourmaux, S.; Kieffer, J. C.; Fujimori, A.; Onoda, M.; Wall, S.; Cavalleri, A. Optical Switching in VO_2 Films by Below-Gap Excitation. *Appl. Phys. Lett.* **2008**, *92*, 181904.
(4) Nakano, M.; Shibuya, K.; Ogawa, N.; Hatano, T.; Kawasaki, M.; Iwasa, Y.; Tokura, Y. Infrared-Sensitive Electrochromic Device Based on VO_2. *Appl. Phys. Lett.* **2013**, *103*, 153503.
(5) Heckingbottom, R.; Linnett, J. W. Structure of Vanadium Dioxide. *Nature* **1962**, *194*, 678.
(6) Wu, J. M.; Chen, Y. R.; Kao, W. T. Ultrafine ZnO Nanoparticles/Nanowires Synthesized on a Flexible and Transparent Substrate: Formation, Water Molecules, and Surface Defect Effects. *ACS Appl. Mater. Interfaces* **2014**, *6*, 487−494.
(7) Wu, J. M.; Fang, C. W.; Lee, L. T.; Yeh, H. H.; Lin, Y. H.; Yeh, P. H.; Tsai, L. N.; Lin, L. J. Photoresponsive and Ultraviolet to Visible-Light Range Photocatalytic Properties of ZnO:Sb Nanowires. *J. Electrochem. Soc.* **2011**, *158*, K6−K10.
(8) Wu, J. M.; Chen, Y. R.; Lin, Y. H. Rapidly Synthesized ZnO Nanowires by Ultraviolet Decomposition Process in Ambient Air for Flexible Photodetector. *Nanoscale* **2011**, *3*, 1053−1058.
(9) Yang, Q.; Wang, W. H.; Xu, S.; Wang, Z. L. Enhancing Light Emission of ZnO Microwire-Based Diodes by Piezo-Phototronic Effect. *Nano Lett.* **2011**, *11*, 4012−4017.
(10) Yang, Q.; Guo, X.; Wang, W. H.; Zhang, Y.; Xu, S.; Lien, D. H.; Wang, Z. L. Enhancing Sensitivity of a Single ZnO Micro-/Nanowire Photodetector by Piezo-Phototronic Effect. *ACS Nano* **2010**, *4*, 6285−6291.
(11) Rigutti, L.; Tchernycheva, M.; Bugallo, A. D.; Jacopin, G.; Julien, F. H.; Zagonel, L. F.; March, K.; Stephan, O.; Kociak, M.; Songmuang, R. Ultraviolet Photodetector Based on GaN/AlN Quantum Disks in a Single Nanowire. *Nano Lett.* **2010**, *10*, 2939−2943.
(12) Wu, J. M.; Kuo, C. H. Ultraviolet Photodetectors Made from SnO_2 Nanowires. *Thin Solid Films* **2009**, *517*, 3870−3873.
(13) Wu, J. M.; Hsu, G. K.; Yeh, H. H.; Lin, H. C. Metallic Zinc Nanowires Effect in High-Performance Photoresponsive and Photocatalytic Properties of Composite Zinc Stannate Nanowires. *J. Electrochem. Soc.* **2012**, *159*, H497−H501.
(14) Geim, A. K.; Novoselov, K. S. The Rise of Graphene. *Nat. Mater.* **2007**, *6*, 183−191.
(15) Radisavljevic, B.; Radenovic, A.; Brivio, J.; Giacometti, V.; Kis, A. Single-Layer MoS_2 Transistors. *Nat. Nanotechnol.* **2011**, *6*, 147−150.
(16) Sangwan, V. K.; Arnold, H. N.; Jariwala, D.; Marks, T. J.; Lauhon, L. J.; Hersam, M. C. Low-Frequency Electronic Noise in Single-Layer MoS_2 Transistors. *Nano Lett.* **2013**, *13*, 4351−4355.
(17) Hu, P. A.; Wang, L. F.; Yoon, M.; Zhang, J.; Feng, W.; Wang, X. N.; Wen, Z. Z.; Idrobo, J. C.; Miyamoto, Y.; Geohegan, D. B.; Xiao, K. Highly Responsive Ultrathin GaS Nanosheet Photodetectors on Rigid and Flexible Substrates. *Nano Lett.* **2013**, *13*, 1649−1654.
(18) Khan, M. A.; Kuznia, J. N.; Olson, D. T.; Vanhove, J. M.; Blasingame, M.; Reitz, L. F. High-Responsivity Photoconductive Ultraviolet Sensors Based on Insulating Single-Crystal GaN Epilayers. *Appl. Phys. Lett.* **1992**, *60*, 2917−2919.
(19) Balog, R.; Jorgensen, B.; Nilsson, L.; Andersen, M.; Rienks, E.; Bianchi, M.; Fanetti, M.; Laegsgaard, E.; Baraldi, A.; Lizzit, S.; Sljivancanin, Z.; Besenbacher, F.; Hammer, B.; Pedersen, T. G.; Hofmann, P.; Hornekaer, L. Bandgap Opening in Graphene Induced by Patterned Hydrogen Adsorption. *Nat. Mater.* **2010**, *9*, 315−319.
(20) Samuels, A. J.; Carey, J. D. Molecular Doping and Band-Gap Opening of Bilayer Graphene. *ACS Nano* **2013**, *7*, 2790−2799.
(21) Wang, S. H.; Tsai, T. Y.; Chang, S. J.; Weng, W. Y.; Chang, S. P.; Hsu, C. L. Enhanced Field Emission of TiO_2 Nanowires With UV Illumination. *IEEE Electron Device Lett.* **2014**, *35*, 123−125.
(22) Xie, F. X.; Choy, W. C. H.; Sha, W. E. I.; Zhang, D.; Zhang, S. Q.; Li, X. C.; Leung, C. W.; Hou, J. H. Enhanced Charge Extraction in Organic Solar Cells Through Electron Accumulation Effects Induced by Metal Nanoparticles. *Energy Environ. Sci.* **2013**, *6*, 3372−3379.
(23) Ko, C.; Yang, Z.; Ramanathan, S. Work Function of Vanadium Dioxide Thin Films across the Metal−Insulator Transition and the Role of Surface Nonstoichiometry. *ACS Appl. Mater. Interfaces* **2011**, *3*, 3396−401.
(24) Rigutti, L.; Tchernycheva, M.; Bugallo, A. D.; Jacopin, G.; Julien, F. H.; Zagonel, L. F.; March, K.; Stephan, O.; Kociak, M.; Songmuang, R. Ultraviolet Photodetector Based on GaN/AlN Quantum Discs in a Single Nanowire. *Nano Lett.* **2010**, *10*, 4284−4284.
(25) Guo, F. W.; Yang, B.; Yuan, Y. B.; Xiao, Z. G.; Dong, Q. F.; Bi, Y.; Huang, J. S. A Nanocomposite Ultraviolet Photodetector Based on Interfacial Trap-Controlled Charge Injection. *Nat. Nanotechnol.* **2012**, *7*, 798−802.
(26) Konstantatos, G.; Badioli, M.; Gaudreau, L.; Osmond, J.; Bernechea, M.; de Arquer, F. P. G.; Gatti, F.; Koppens, F. H. L. Hybrid Graphene−Quantum Dot Phototransistors with Ultrahigh Gain. *Nat. Nanotechnol.* **2012**, *7*, 363−368.
(27) Wei Tian, C. Z.; Zhai, T.; Li, S.-L.; Wang, Xi; Liu, J.; Jie, X.; Liu, D.; Liao, M.; Koide, Y.; Golberg, D.; Bando, Y. Flexible Ultraviolet Photodetectors with Broad Photoresponse Based on Branched ZnS−ZnO Heterostructure Nanofilms. *Adv. Mater.* **2014**, *26*, 3088−3093.
(28) Wu, J. M.; Shih, H. C.; Wu, W. T.; Tseng, Y. K.; Chen, I. C. Thermal Evaporation Growth and The Luminescence Property of TiO_2 Nanowires. *J. Cryst. Growth* **2005**, *281*, 384−390.
(29) Zhai, T. Y.; Li, L.; Ma, Y.; Liao, M. Y.; Wang, X.; Fang, X. S.; Yao, J. N.; Bando, Y.; Golberg, D. One-Dimensional Inorganic Nanostructures: Synthesis, Field-Emission and Photodetection. *Chem. Soc. Rev.* **2011**, *40*, 2986−3004.
(30) Zhang, Y. Z.; Liu, T.; Meng, B.; Li, X. H.; Liang, G. Z.; Hu, X. N.; Wang, Q. J. Broadband High Photoresponse from Pure Monolayer Graphene Photodetector. *Nat. Commun.* **2013**, *4*, 1881.
(31) Manekkathodi, A.; Lu, M. Y.; Wang, C. W.; Chen, L. J. Direct Growth of Aligned Zinc Oxide Nanorods on Paper Substrates for Low-Cost Flexible Electronics. *Adv. Mater.* **2010**, *22*, 4059−4063.
(32) Wu, J. M.; Shih, H. C.; Wu, W. T. Formation and Photoluminescence of Single-Crystalline Rutile TiO_2 Nanowires Synthesized by Thermal Evaporation. *Nanotechnology* **2006**, *17*, 105−109.
(33) Mukherjee, B.; Cai, Y. Q.; Tan, H. R.; Feng, Y. P.; Tok, E. S.; Sow, C. H. NIR Schottky Photodetectors Based on Individual Single-Crystalline GeSe Nanosheet. *ACS Appl. Mater. Interfaces* **2013**, *5*, 9594−9604.
(34) Xia, F. N.; Mueller, T.; Lin, Y. M.; Valdes-Garcia, A.; Avouris, P. Ultrafast Graphene Photodetector. *Nat. Nanotechnol.* **2009**, *4*, 839−843.
(35) Yin, Z. Y.; Li, H.; Li, H.; Jiang, L.; Shi, Y. M.; Sun, Y. H.; Lu, G.; Zhang, Q.; Chen, X. D.; Zhang, H. Single-Layer MoS_2 Phototransistors. *ACS Nano* **2012**, *6*, 74−80.
(36) Hu, P. A.; Wen, Z. Z.; Wang, L. F.; Tan, P. H.; Xiao, K. Synthesis of Few-Layer GaSe Nanosheets for High Performance Photodetectors. *ACS Nano* **2012**, *6*, 5988−5994.
(37) Sohn, J. I.; Joo, H. J.; Porter, A. E.; Choi, C. J.; Kim, K.; Kang, D. J.; Welland, M. E. Direct Observation of The Structural Component of The Metal-Insulator Phase Transition and Growth Habits of Epitaxially Grown VO_2 Nanowires. *Nano Lett.* **2007**, *7*, 1570−4.
(38) Wu, J. M.; Chen, C. Y.; Zhang, Y.; Chen, K. H.; Yang, Y.; Hu, Y.; He, J. H.; Wang, Z. L. Ultrahigh Sensitive Piezotronic Strain Sensors Based on a $ZnSnO_3$ Nanowire/Microwire. *ACS Nano* **2012**, *6*, 4369−4374.

(39) Wu, J. M.; Xu, C.; Zhang, Y.; Wang, Z. L. Lead-Free Nanogenerator Made from Single $ZnSnO_3$ Microbelt. *ACS Nano* **2012**, *6*, 4335−4340.
(40) Guiton, B. S.; Gu, Q.; Prieto, A. L.; Gudiksen, M. S.; Park, H. Single-Crystalline Vanadium Dioxide Nanowires with Rectangular Cross Sections. *J. Am. Chem. Soc.* **2005**, *127*, 498−499.
(41) Li, Y. M.; Ji, S. D.; Gao, Y. F.; Luo, H. J.; Kanehira, M. Core-Shell VO_2@TiO_2 Nanorods That Combine Thermochromic and Photocatalytic Properties for Application as Energy-Saving Smart Coatings. *Sci. Rep* **2013**, *3*, 1370.
(42) Wu, J. M. A Room Temperature Ethanol Sensor Made from P-type Sb-doped SnO_2 Nanowires. *Nanotechnology* **2010**, *21*, 235501.
(43) Liu, X.; Gu, L.; Zhang, Q.; Wu, J.; Long, Y.; Fan, Z. All-Printable Band-Edge Modulated ZnO Nanowire Photodetectors with Ultra-High Detectivity. *Nat. Commun.* **2014**, *5*, 4007.
(44) Park, W.; Jo, G.; Hong, W. K.; Yoon, J.; Choe, M.; Lee, S.; Ji, Y.; Kim, G.; Kahng, Y. H.; Lee, K.; Wang, D. L.; Lee, T. Enhancement in The Photodetection of ZnO Nanowires by Introducing Surface-Roughness-Induced Traps. *Nanotechnology* **2011**, *22*, 205204.
(45) Binet, F.; Duboz, J. Y.; Rosencher, E.; Scholz, F.; Harle, V. Mechanisms of Recombination in GaN Photodetectors. *Appl. Phys. Lett.* **1996**, *69*, 1202−1204.
(46) Liu, S.; Wei, Z. M.; Cao, Y.; Gan, L.; Wang, Z. X.; Xu, W.; Guo, X. F.; Zhu, D. B. Ultrasensitive Water-Processed Monolayer Photodetectors. *Chem. Sci.* **2011**, *2*, 796−802.
(47) Shao, D.; Yu, M.; Sun, H.; Hu, T.; Lian, J.; Sawyer, S. High Responsivity, Fast Ultraviolet Photodetector Fabricated from ZnO Nanoparticle−Graphene Core−Shell Structures. *Nanoscale* **2013**, *5*, 3664−7.
(48) Qin, L. Q.; Shing, C.; Sawyer, S. Metal-Semiconductor-Metal Ultraviolet Photodetectors Based on Zinc-Oxide Colloidal Nanoparticles. *IEEE Electron Device Lett.* **2011**, *32*, 51−53.
(49) Zhou, J.; Fei, P.; Gu, Y. D.; Mai, W. J.; Gao, Y. F.; Yang, R.; Bao, G.; Wang, Z. L. Piezoelectric-Potential-Controlled Polarity-Reversible Schottky Diodes and Switches of ZnO Wires. *Nano Lett.* **2008**, *8*, 3973−3977.
(50) Hu, Y. F.; Zhou, J.; Yeh, P. H.; Li, Z.; Wei, T. Y.; Wang, Z. L. Supersensitive, Fast-Response Nanowire Sensors by Using Schottky Contacts. *Adv. Mater.* **2010**, *22*, 3327−3332.
(51) Cheng, Y.; Wong, T. L.; Ho, K. M.; Wang, N. The Structure and Growth Mechanism of VO_2 Nanowires. *J. Cryst. Growth* **2009**, *311*, 1571−1575.